PsbU Provides a Stable Architecture for the Oxygen-Evolving System in Cyanobacterial Photosystem II †

5 AUTHORS, INCLUDING:

Yasuhiro Kashino
University of Hyogo

91 PUBLICATIONS   2,013 CITATIONS

SEE PROFILE

Ichiro Terashima
The University of Tokyo

155 PUBLICATIONS   6,983 CITATIONS

SEE PROFILE

PsbU Provides a Stable Architecture for the Oxygen-Evolving System in Cyanobacterial Photosystem II[†]

Natsuko Inoue-Kashino,[‡,§,||] Yasuhiro Kashino,*[,‡,||] Kazuhiko Satoh,[||] Ichiro Terashima,[§] and Himadri B. Pakrasi[‡]

Department of Biology, Washington University, St. Louis, Missouri 63130, Department of Biology, Graduate School of Science, Osaka University, Toyonaka, Osaka 560-0043, Japan, and Department of Life Science, Graduate School of Life Science, University of Hyogo, Ako-gun, Hyogo 678-1297, Japan

ABSTRACT: PsbU is a lumenal peripheral protein in the photosystem II (PS II) complex of cyanobacteria and red algae. It is thought that PsbU is replaced functionally by PsbP or PsbQ in plant chloroplasts. After the discovery of PsbP and PsbQ homologues in cyanobacterial PS II [Thornton et al. (2004) *Plant Cell 16*, 2164−2175], we investigated the function of PsbU using a *psbU* deletion mutant (ΔPsbU) of *Synechocystis* 6803. In contrast to the wild type, ΔPsbU did not grow when both Ca^{2+} and Cl^- were eliminated from the growth medium. When only Ca^{2+} was eliminated, ΔPsbU grew well, whereas when Cl^- was eliminated, the growth rate was highly suppressed. Although ΔPsbU grew normally in the presence of both ions under moderate light, PS II-related disorders were observed as follows. (1) The mutant cells were highly susceptible to photoinhibition. (2) Both the efficiency of light utilization under low irradiance and the chlorophyll-specific maximum rate of oxygen evolution in ΔPsbU cells were 60% lower than those of the wild type. (3) The decay of the S2 state in ΔPsbU cells was decelerated. (4) In isolated PS II complexes from ΔPsbU cells, the amounts of the other three lumenal extrinsic proteins and the electron donation rate were drastically decreased, indicating that the water oxidation system became significantly labile without PsbU. Furthermore, oxygen-evolving activity in ΔPsbU thylakoid membranes was highly suppressed in the absence of Cl^-, and 60% of the activity was restored by NO_3^- but not by SO_4^{2-}, indicating that PsbU had functions other than stabilizing Cl^-. On the basis of these results, we conclude that PsbU is crucial for the stable architecture of the water-splitting system to optimize the efficiency of the oxygen evolution process.

The photosynthetic electron transport system in oxygenic photosynthesis converts light energy to biochemical energy and consists of three major large membrane protein complexes, namely, photosystem I (PS I),[1] cytochrome (cyt) b_6f, and photosystem II (PS II) complexes (*1*). Recently, all of these complexes were crystallized, and the structural models were presented at high resolution [2.5 Å in cyanobacterial PS I (*2*), 4.4 Å in plant PS I (*3*), 3.0 and 3.1 Å in cyt b_6f (*4*, *5*), and 3.2−3.8 Å in PS II (*6−9*)]. Among these complexes, PS II is the most integrated membrane protein complex,

which consists of over 20 distinctive membrane proteins, three lumenal extrinsic proteins, and several cofactors (*6*, *8*, *10*, *11*). On the basis of this structure, PS II extracts electrons from water molecules and exhausts molecular oxygen. Although both cyanobacterial and plant PS II complexes contain three lumenal extrinsic proteins that play important roles in PS II-mediated water oxidation, only one of them (PsbO) is shared in both complexes; PsbO, PsbU, and PsbV in cyanobacterial PS II and PsbO, PsbP, and PsbQ in plant PS II (*10*). Until now, no similarity was found in the amino acid sequences and structures between the residual two proteins (PsbU and PsbV vs PsbP and PsbQ) (*6*, *11−13*).

PsbU was first found as a 9 kDa lumenal extrinsic protein in a highly active PS II complex isolated from *Phormidium laminosum*, which assisted oxygen evolution with PsbO manganese-stabilizing protein (*14*, *15*). Another peripheral protein, cytochrome *c*-550, was found in *Anacystis nidulans* and *Microcystis aeruginosa* (*16*, *17*) and was attributed later as an important lumenal extrinsic protein of cyanobacterial PS II (PsbV) (*18*, *19*). Both of the corresponding genes (*psbU* and *psbV*) were then found in all cyanobacterial genomes analyzed except for two strains of *Prochlorophytes*, *Prochlorococcus marinus* MED4 and *P. marinus* SS120 (*20*). Genetic and biochemical investigations on these two proteins have been performed in the past decade. Shen et al. genetically deleted *psbU* and/or *psbV* genes from the

* Address correspondence to this author at the University of Hyogo. Phone/Fax: +81 791 58 0185. E-mail: kashino@sci.u-hyogo.ac.jp.
‡ Washington University.
§ Osaka University.
|| University of Hyogo.

[1] Abbreviations: α, initial slope in light curve; Chl, chlorophyll; CP47 and CP43, peripheral Chl binding proteins of 47 and 43 kDa in PS II; cyt, cytochrome; DCBQ, dichloro-*p*-benzoquinone; DCMU, 3-(3,4-dichlorophenyl)-1,1-dimethylurea; F_0, F_m, and F_v, initial, maximal, and variable fluorescence yield; I_k, intensity at the onset of light saturation; Km[r], Gm[r], and Em[r], kanamycin-, gentamycin-, and erythromycin-resistance cartridges, respectively; PS I and PS II, photosystem I and II; MES, 2-(*N*-morpholino)ethanesulfonic acid monohydrate; P_{max}, maximum photosynthetic rate.

cyanobacterium *Synechocystis* sp. PCC 6803 and investigated the effects of these deletions (*21*, *22*). Without PsbV, the cells did not grow autotrophically when Ca^{2+} or Cl^- was eliminated from the growth media. Furthermore, the *psbV* deletion mutant (ΔPsbV) showed unusual S-state transitions and exhibited an unstable oxygen-evolving activity (*22*). Although Shen et al. also detected modification of the S2 state in the *psbU* deletion mutant (ΔPsbU) by examining thermoluminescence, they did not observe a remarkable impairment in the growth rates under any growth conditions tested (normal BG11, BG11$-Ca^{2+}$, BG11$-Cl^-$) (*21*, *22*). On the basis of these results, they concluded that PsbV was important for the stability and function of the manganese cluster in cyanobacterial PS II, while they only suggested that PsbU would play roles in maintaining the normal S-state transitions and in the maximum affinity of PS II for Ca^{2+} and Cl^- ions (*21*, *22*).

Similar to the extrinsic proteins in higher plant PS II (PsbO, PsbP, and PsbQ), PsbU and PsbV can also be removed from isolated PS II by high concentrations of salts (*11*, *18*, *19*). Using isolated cyanobacterial and red algal PS II complexes, Shen and his group demonstrated that, without PsbU or PsbV, PS II complexes require high concentrations of Ca^{2+} and Cl^- for the high oxygen-evolving activity (*19*, *23*). PsbV can be reconstituted alone to the salt-washed PS II complexes, whereas the assembly of PsbV and PsbO to the salt-washed PS II is a prerequisite for the effective reconstitution of PsbU (*19*). With regard to the binding characteristics, PsbU and PsbV correspond to PsbQ and PsbP in higher plant PS II (*24*). On the basis of these biochemical analyses, it is generally accepted that the entities and functions of PsbU and PsbV proteins were replaced with PsbQ and PsbP proteins, respectively, during the evolutional process (*18*, *19*, *25*, *26*).

Recently, we have found two proteins in the cyanobacterial PS II complexes from *Synechocystis* 6803 which have homology to plant PsbP and PsbQ (sequence identities are 27.3% and 32.9% for PsbP and PsbQ between *Synechocystis* 6803 and *Arabidopsis*, respectively) (*11*, *27*) although these proteins are not found in the reported three-dimensional PS II structure from thermophilic cyanobacteria (*6*−*9*). Genome information also supports the presence of PsbP and PsbQ homologues in several cyanobacteria (*20*, *27*). In addition, Summerfield et al. (*28*) demonstrated the association of the PsbQ homologue to the PS II complex and the importance of this protein for PS II stability in *Synechocystis* 6803 (*28*), and Ohta et al. reported the presence of a protein homologous to plant PsbQ in a primitive red alga, *Cyanidium caldarium* (*29*). These findings of PsbP and PsbQ in cyanobacteria and PsbQ in red algae throw doubt on the above-mentioned hypothesis that PsbU and PsbV were functionally and physically replaced by PsbP and PsbQ during the evolutional process to plant chloroplasts (*25*). Therefore, the functions of PsbU and PsbV in relation to those of PsbQ and PsbP should be reexamined. In this study, we conducted detailed analyses to clarify the function of PsbU using the deletion mutant of the *psbU* gene (ΔPsbU). Since Ca^{2+} and Cl^- are well-known to be essential for oxygen evolution, we, first, examined the growth of cells under the Ca^{2+}- and/or Cl^--depleted conditions. The Cl^- depletion resulted in a severer suppression of growth rate in ΔPsbU cells than the absence of Ca^{2+}. We also found that ΔPsbU cells were more

susceptible to photoinhibition. The fluorescence rise kinetics showed that water oxidation in PS II was slowed in ΔPsbU mutant cells grown in normal BG11 and further if they were grown without Cl^-. Light curves exhibited that the efficiency of oxygen evolution in ΔPsbU cells was remarkably lower than that of the wild type. The lifetime of the S2 state in ΔPsbU cells grown in normal BG11 was prolonged. The absence of PsbU did not affect the stoichiometry of PS II and PS I. In isolated thylakoids, oxygen-evolving activity was highly suppressed, and part of the activity was restored by the addition of monovalent anion, NO_3^-. In the PS II complexes isolated from ΔPsbU cells by highly mild conditions, the amounts of the PsbO, PsbQ, and PsbV proteins and the electron donation rate were drastically decreased. Unlike the original proposal for PsbU function (*10*) as affinity sites for Ca^{2+} and/or Cl^-, the present results clearly indicate that PsbU is important in construction of a stable architecture of the oxygen-evolving system in PS II.

MATERIALS AND METHODS

Cyanobacterial Strains and Growth Conditions. *Synechocystis* 6803 cells (the wild type and the mutants which lacked PsbU or PsbO) were grown on a rotary shaker at 30 °C under 50 μmol of photons·m^{-2}·s^{-1} of white light in BG11 medium (*30*) using plastic tissue culture plates with 12 wells (CELLSTAR; Greiner Bio-One, Frickenhausen, Germany) with 3 mL triplicates for each medium condition to measure the growth rates. The cells were grown with bubbling air in plastic tissue culture flasks [250 mL (75 cm^2); Corning, Corning, NY] for the measurement of oxygen evolution. Prior to growth measurements, cells that were cultivated in normal BG11 for 3 days were washed three times with CaCl$_2$-depleted BG11 medium (BG11$-$CaCl$_2$) and resuspended in the same medium. They were then diluted into the appropriate media as described below to OD$_{730nm}$ = 0.05−0.06.

Ca^{2+}- and/or Cl^--depleted BG11 medium was prepared in plastic ware to exclude contamination of ions. Media were prepared with either Ca^{2+} [240 μM Ca(NO$_3$)$_2$] or Cl^- (480 μM NaCl). Growth was monitored by measuring OD$_{730nm}$ on a MQX200 μQuant Universal microplate spectrophotometer with operating software KC4 (Bio-Tek Instruments, Winooski, VT) and 96-well tissue culture plates (150 μL from each sample). The accuracy of this monitoring system was checked in advance by a DW2000 spectrophotometer (SLM-Aminco, Urbana, IL).

Gene Cloning and Isolation of Mutants. The upstream and downstream regions [298488−297889 and 297469−296961 (Cyanobase, http://www.kazusa.or.jp/cyanobase/)] of the *sll1194* (*psbU*) gene of *Synechocystis* 6803 were amplified by PCR using the following oligonucleotide primers (Figure 1A): 5′-CGAAGCTTTGGAAAATAATG-3′ (primer P1) and 5′-GAATTGTCTCCTATAACCAA-3′ (primer P2) for 298488−297889 and 5′-GCGCGG<u>GAGCTC</u>CATTATTCAT-TGTCTAGATA-3′ (primer P3) and 5′-GCGCGG<u>GAGCTC</u>-TTTTGATCAGTCATTTGGAA-3′ (primer P4) with *Sac*I restriction sites (underlined sequences in the primers) for 297469−296961. The PCR product from the upstream region (#1 in Figure 1) was cloned into TA cloning vector pGEM-T (Promega, Madison, WI) (Figure 1B). Then, the PCR product from the downstream region (#2 in Figure 1), which had been processed by *Sac*I, was inserted into the *Sac*I site of
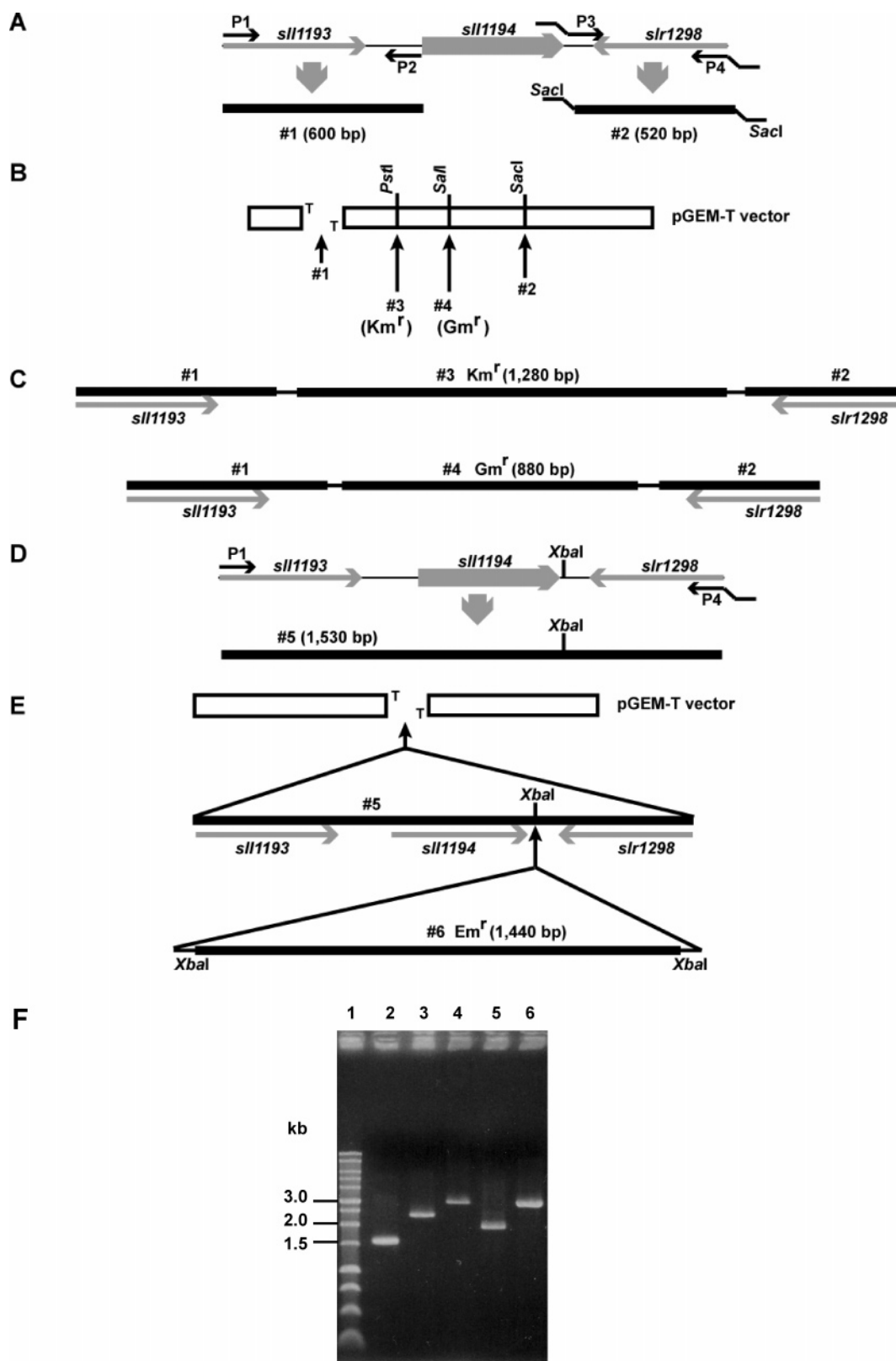
FIGURE 1: Scheme for making constructs to delete and complement the *psbU* gene (A–E). The solid bars which are expressed by #1, #2, and #5 are the PCR products from genome DNA, and solid bars #3, #4, and #6 are the antibiotic-resistance cartridges. Km[r], Gm[r], and Em[r] are the kanamycin-, gentamycin-, and erythromycin-resistance cartridges, respectively. Segregation of the deletion and complementation mutations of the *psbU* gene was examined by PCR (F). The PCR products obtained with the P1 and P4 primers using genomic DNA from *Synechocystis* 6803 cells were subjected to electrophoresis. Lanes: 1, 1 kb DNA ladder (Promega, Madison, WI); 2, wild type (1.53 kb); 3, ΔPsbU (2.43 kb); 4, ΔPsbU complement (2.97 kb); 5, ΔPsbU/HT3 (2.04 kb); 6, ΔPsbU/HT3 complement (2.97 kb). Numbers in parentheses are the expected lengths of PCR products. For details, see Materials and Methods.

the resulting plasmid (Figure 1B). The orientation of these two inserts was checked by PCR using the above primers and cleavage by several appropriate restriction enzymes (data not shown). A kanamycin-resistance cartridge (*31*) (Km[r], #3

in Figure 1) or a gentamycin-resistance cartridge (*32*) (Gm[r], #4 in Figure 1) was introduced into the *Pst*I site or *Sal*I site of the resulting plasmid, respectively, which was located between the two inserts (Figure 1B). These two constructs (Figure 1C) were used to delete the *psbU* gene from the wild-type and HT3 (Km[r]) strains of *Synechocystis* 6803, respectively. The HT3 strain, which has a hexahistidine tag on the carboxyl terminus of CP47 (*33*), was a generous gift from Prof. Terry M. Bricker at Louisiana State University. The Km[r] cartridge in the HT3 strain had been inserted into the genomic DNA to select the intended mutation to generate the histidine tag (*33*). The ΔPsbU/wild-type strain which carries the Km[r] cartridge was used from Figure 2 through Figure 6 and all figures in Supporting Information, and the ΔPsbU/HT3 strain which carries both the Km[r] and Gm[r] cartridges was used in Figures 7 and 8. To complement the deletion of the *psbU* gene, the region including the *psbU* gene was amplified by PCR using primers P1 and P4 (Figure 1D). This region (#5 in Figure 1D) was cloned into the TA cloning vector pGEM-T (Figure 1E). The erythromycin-resistance cartridge (*34*) (Em[r], #6 in Figure 1) was then inserted into the *Xba*I site at 38 bp downstream of *sll1194* in the resulting plasmid (Figure 1E). Accordingly, the complemented strain from ΔPsbU/wild-type carries the Em[r] cartridge. This complemented strain was used in Figure 5. The ΔPsbO mutant was engineered by inserting a spectino-mycin-resistance cassette in a *Bam*HI site of the *psbO* (sll0427) gene of *Synechocystis* 6803. The accuracy of all PCR products used in Figure 1 was checked by sequencing.

The complete segregation of the mutation was demonstrated by PCR (Figure 1F).

Isolation of Thylakoid Membranes and PS II Complexes. Thylakoid membranes from wild-type and ΔPsbU strains and the PS II complexes from the HT3 and ΔPsbU/HT3 strains were isolated as previously described (*11*). Thylakoid membranes were also prepared with or without Cl⁻ ions from wild-type and ΔPsbU stains. The cells were broken by glass beads as was described in ref *11*, and then the membranes were washed twice by a solution containing 50 mM 2-(*N*-morpholino)ethanesulfonic acid monohydrate (MES)−NaOH (pH 6.5), 10 mM MgCl₂, 5 mM CaCl₂, and 1 M betaine or a solution containing 50 mM MES−NaOH (pH 6.5), 10 mM MgSO₄, 5 mM CaSO₄, and 1 M betaine. The resulting thylakoid membranes were resuspended in the respective solutions. The measured Cl⁻ concentration was 36.4 mM for the former solution and less than the detectable limit (<20 μM) for the latter solution.

Electrophoresis and Immunodetection. SDS−PAGE and immunoblotting were performed using a gel containing 20% acrylamide and 6 M urea (Figures S3 and S4, Supporting Information) or a gel containing a 18−24% acrylamide gradient and 6 M urea (Figure 7) (*35, 36*). Antisera raised against CP1-e (PsaA/B), CP47, CP43 (*37*), PsbO (kindly provided from Prof. Louis A. Sherman at Purdue University), and PsbQ (*27*) were used, and the respective cross-reactive bands were detected by chemiluminescence (WestPico; Pierce, Rockford, IL). Heme was detected by chemiluminescence using WestFemto (Pierce) reagents after electrophoresis (*36*).

Oxygen Evolution Assays. Cells that had grown for 3 days in normal BG11 medium were washed and resuspended in fresh BG11 at 10 μg of chlorophyll (Chl)/mL and were used

for the assay of PS II-mediated activity in whole cells. Isolated PS II samples and thylakoid membranes were used at 2 μg of Chl/mL and 10 μg of Chl/mL, respectively, in a buffer containing 50 mM MES−NaOH (pH 6.0), 10 mM MgCl₂, 5 mM CaCl₂, and 0.5 M sucrose for PS II complexes and 50 mM MES−NaOH (pH 6.5), 10 mM MgCl₂, 5 mM CaCl₂, and 1 M betaine for thylakoids. The Cl⁻-depleted reaction mixture was prepared using sulfate salts. Chl concentration was determined by the method of Porra et al. (*38*). Steady-state oxygen evolution was measured with a Clark-type electrode in the presence of 1 mM 2,6-dichloro-*p*-benzoquinone (DCBQ) for PS II complexes and 0.5 mM 2,5-DCBQ for thylakoids as an electron acceptor. An Oriel 66180 halogen lamp (Stratford, CT) supplied actinic light through an OG 570 long-pass filter (Schott, Mainz, Germany). Light intensity was adjusted by use of a neutral density filter and determined using a quantum photometer (Licor, Inc., Lincoln, NE). The photosynthetic rate (*P*) was plotted against the light intensity (*I*), and the curve was fitted to the equations described below (*39*) using a data analysis program, KaleidaGraph version 3.6 (Synergy Software, Reading, PA):

$$P = P_{max}[1 - \exp(-\alpha I/P_{max})]$$

$$I_k = P_{max}/\alpha$$

where P_{max} is the maximal photosynthetic rate, α is the initial slope (light utilization efficiency), and I_k is the irradiance at the onset of light saturation.

The lifetimes of S2 and S3 were measured on a bare platinum electrode (Artisian Scientific Co., Urbana, IL) based on a procedure described in ref *40* with modification. Cells that were dark adapted for 10 min were illuminated by a single activation flash followed by another 10 min dark incubation. A single activation flash (for S2 measurement) or two consecutive actinic flashes with an interval of 300 ms (for S3 measurement) were then supplied, followed by a variable period of dark incubation. This period, which included the polarization period of 30 s, was the delay time for the analysis of S2 and S3 decay kinetics (the shortest delay time was 30 s). A train of 50 flashes at 3.33 Hz was supplied after this delay time. The oxygen yields at the second (for S2) or the first flash (for S3) during this 50 flash series were used for the analysis of the lifetimes of S2 and S3 states.

The calculation method of the decay kinetics of S2 and S3 states was modified from that described previously (*40*). The difficulty in obtaining an accurate fit is a result of the absence of the initial values of S2 or S3. In the report by Young et al. (*40*), the value at 0 s was taken as the initial value. However, time 0 s should have been designated as 20 s, because Young et al. waited for 20 s for polarization of the electrode after the delay time (30 s in our experiments), which was inevitable with this system. Thus, the lifetime of the S2 state was calculated as follows. (1) The 4-fold value of the average oxygen yield at the last four flashes (47−50th flashes) was designated as the maximum value for the oxygen yield, and the oxygen yield at every flash was normalized against this value. This is a reasonable assumption because at approximately 50 flashes, the oscillation is damped and the S-states are evenly distributed into four

Table 1: S-State Distribution and Parameters Determined by Analyzing Oscillation Patterns of Flash Oxygen Yield[a]

	S-state distribution				S-state parameters	
	S0 (%)	S1 (%)	S2 (%)	S3 (%)	miss hit (%)	double hit (%)
wild type	26 (1.6)	71 (1.8)	1.7 (0.27)	0.94 (0.59)	12 (0.59)	2.0 (0.047)
ΔPsbU	30 (2.1)	64 (3.4)	1.5 (1.5)	4.0 (0.90)	14 (0.90)	2.0 (0.40)

[a] The S-state parameters were analyzed using a simple four-step, homogeneous model (*70*). Cells were grown in normal BG11 medium. Numbers in parentheses are standard deviations ($n = 3$ for wild type and $n = 7$ for ΔPsbU).

states, and the oxygen yield at such flashes can be considered as one-quarter of the maximum yield. (2) The relative population of the S1 state in the dark-adapted cells, which was determined by analyzing the oscillation pattern of the flash oxygen yield (Table 1), was considered as the initial value of the S2 state. This is because only the reaction centers in the S1 state after dark adaptation are responsible for the oxygen yield at the second flash after the delay time. The miss hit was also incorporated, but a double hit was disregarded since it was negligible (Table 1). The amount of S2 ([S2]) after a given delay time (t, which includes the polarization period of 30 s) is expressed as follows if the decay kinetics contains two components (*40*):

$$[S2] = \{[S1]_0(1 - m)\}(1 - m)^2\{p_1 \exp(-q_1 t) + p_2 \exp(-q_2 t)\} = [S1]_0(1 - m)^3\{p_1 \exp(-q_1 t) + p_2 \exp(-q_2 t)\}$$

where $[S1]_0$ is the relative population of S1 after dark adaptation (Table 1), m is the miss hit (Table 1), p_1 and p_2 are distribution factors of the two components ($p_1 + p_2 = 1$), q_1 and q_2 are time constants ($t_{1/2} = \ln 2/q_1$ or $\ln 2/q_2$), $\{[S1]_0(1 - m)\}$ is the relative population of "S2" before the delay time, and $(1 - m)^2$ is a factor originating from the two flashes after the delay time.

Similarly, the lifetime of S3 was calculated from the equation:

$$[S3] = \{[S1]_0(1 - m)^2\}(1 - m)\{p_1 \exp(-q_1 t) + p_2 \exp(-q_2 t)\} = [S1]_0(1 - m)^3\{p_1 \exp(-q_1 t) + p_2 \exp(-q_2 t)\}$$

where $\{[S1]_0(1 - m)^2\}$ is the relative population of "S3" before the delay time and $(1 - m)$ is a factor originating from the single flash after the delay time.

Fluorescence Kinetics. Fluorescence induction kinetics was measured using a double-modulation fluorometer, FL-100 (Photon System Instruments, Brno, Czech Republic), with a built-in analyzing program, FluorWin, at room temperature (*41*). Normal BG11 was used as an assay medium for cells. A solution containing 50 mM MES−NaOH (pH 6.0), 10 mM MgCl₂, 5 mM CaCl₂, 25% glycerol, and 0.04% dodecyl β-D-maltoside was used as an assay medium for the purified PS II. If necessary, 20 μM 3-(3,4-dichlorophenyl)-1,1-dimethyl-lurea (DCMU) was added. The samples were dark adapted for 5 min. The duration of each actinic flash was 5 μs, and the light intensity was one-fifth of the saturating amount (*41*). Alternatively, fluorescence kinetics was measured on a pulse amplitude modulation fluorometer, PAM 101 (Walz GmbH, Effeltrich, Germany), and the fluorescence signal was recorded on a digital oscilloscope, VP-5710A (Panasonic, Osaka, Japan).

Photoinhibition Measurement. Two-day-grown cells were washed and resuspended into a fresh growth medium at 2 μg of Chl/mL. The cells were placed in a water bath (30 °C) in the presence or absence of 100 μg/mL chloramphenicol and were exposed to high light at 500 μmol of photons·m⁻²·s⁻¹ using an Oriel 66187 halogen lamp through a water filter of 6 cm thickness to eliminate the heat from the light source. To assess the recovery after photoinhibition, the cells were washed twice to eliminate chloramphenicol after a 60 min exposure to high light and then placed under 20 μmol of photons·m⁻²·s⁻¹ at 30 °C. At the appropriate time during the photoinhibition and recovery process, small parts of the cells were applied to the fluorescence measurement to take the ratio of variable (F_v) and maximal (F_m) fluorescence. Prior to the measurement by a single saturating flash using the FL-100 (*41*), the cells were incubated for 2 min under the dark.

Spectroscopic Measurements. Absorption spectra at room temperature were measured using a UVIKON 922 spectrophotometer (Kontron, Milan, Italy). Scattering was corrected according to the method described in ref *42*. Fluorescence emission spectra at 77 K were measured using a H-20 UV monochromator (Jobin Yvon, Cedex, France) with a MIC-7 controller (Horiba, Tokyo, Japan) which was operated by the software Okinawa version 2.1 (Horiba, Tokyo, Japan). Chromophores were excited by light supplied by a halogen lamp which was passed through a 4-96 band-pass filter (Corning, Corning, NY). Alternatively, it was measured on a Fluoromax-2 fluorometer (Jobin Yvon, Cedex, France) (*11*).

Chloride Determination. The concentration of Cl⁻ in the media was assayed using a Cl⁻-selective electrode (model 8002-10C; Horiba) with a reference electrode (model 2565A-10T; Horiba) in the presence of 0.1 M KNO₃ as a supporting electrolyte.

RESULTS

Effects of Ca²⁺ and Cl⁻ on Growth. The growth of the wild-type and mutant cells was examined under Ca²⁺- and/or Cl⁻-limited conditions. The growth was also compared with that of the ΔPsbO mutant, which is one of the well-documented cell lines lacking peripheral lumenal proteins (*43−48*). Wild-type cells showed logarithmic growth during the initial ∼20 h and then entered a stationary phase in normal BG11 medium (Figure 2A). The ΔPsbU and ΔPsbO mutant cells grew at almost the same rate as the wild-type cells in the normal BG11 medium, although ΔPsbO cells showed a lag phase. Under Ca²⁺-depleted conditions (Figure 2B), the growth rate of the wild type and the ΔPsbU mutant did not show any remarkable differences, whereas the ΔPsbO mutant cells did not grow during the time tested. The effect of Cl⁻ depletion from the growth medium was drastic in ΔPsbU (Figure 2C); the growth rate of ΔPsbU cells was
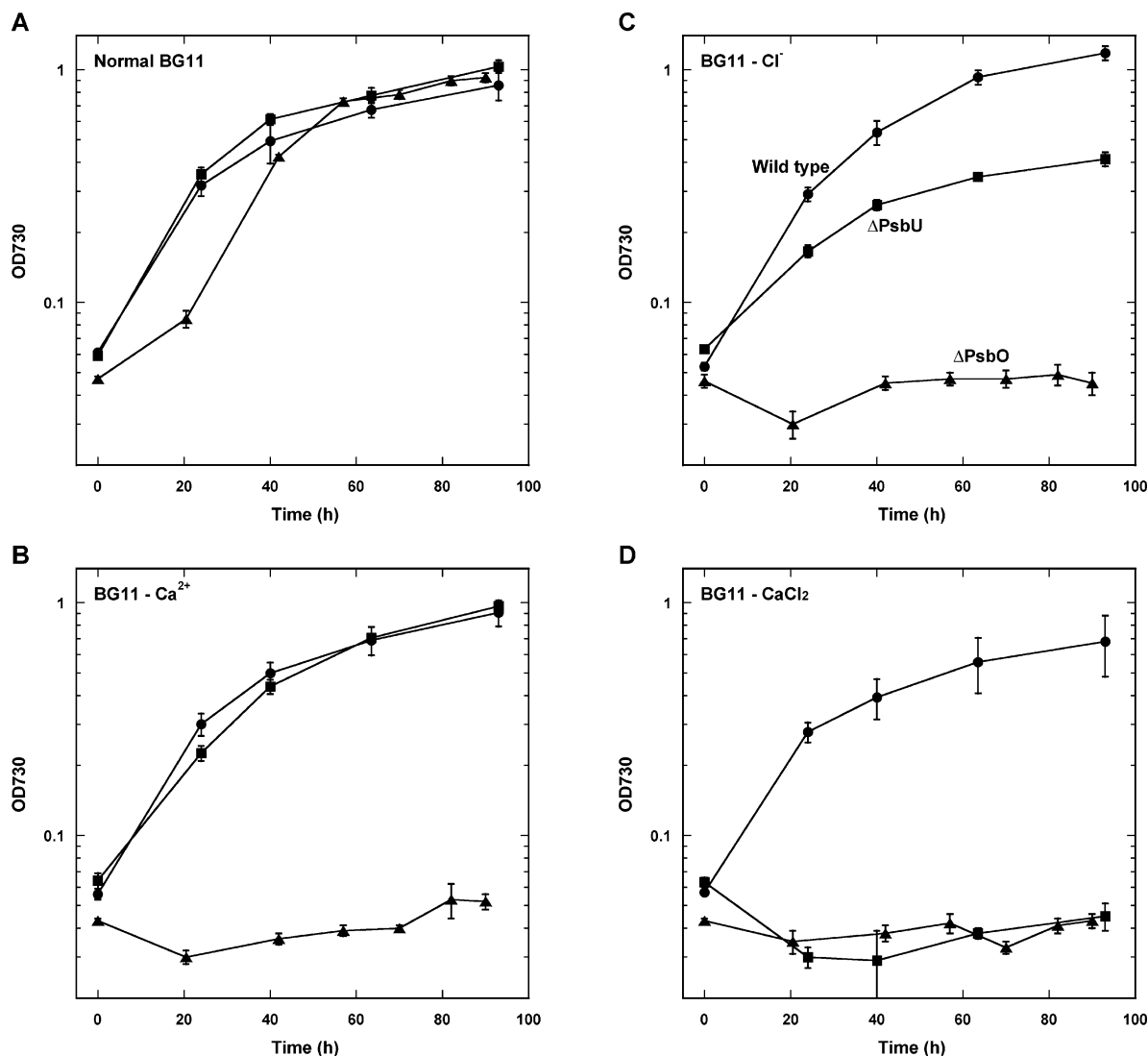
FIGURE 2: Effect of Ca^{2+} and/or Cl^- on cyanobacterial growth. Cells were cultivated in normal BG11 medium for 3 days, washed three times, and resuspended in $BG11-CaCl_2$. They were then diluted to $OD_{730nm} \approx 0.06-0.07$ into BG11 (panel A), $BG11-Ca^{2+}$ (panel B), $BG11-Cl^-$ (panel C), or $BG11-CaCl_2$ medium (panel D). Cells were grown on a rotary shaker at 30 °C under 50 μmol of photons·m^{-2}·s^{-1} for each medium condition. Key: solid circle, wild type; solid square, ΔPsbU; solid triangle, ΔPsbO. Error bars show the standard deviation ($n = 3$). Cl^- concentration in $BG11-Cl^-$ and $BG11-CaCl_2$ media was less than the detectable limit (<20 μM).

suppressed more markedly than that of the wild type. The ΔPsbO cells did not grow under Cl^--depleted conditions (Figure 2C). When Ca^{2+} and Cl^- were depleted (Figure 2D), the ΔPsbU mutant and the ΔPsbO mutant were unable to grow.

Sensitivity to Photoinhibition in Cells. The PS II activity in cells determined by the F_v/F_m value gradually decreased at the same rate in both the wild type and the ΔPsbU mutants in the absence of chloramphenicol under a light intensity of 500 μmol of photons·m^{-2}·s^{-1} (Figure 3). After being washed, the cells were placed under low light (20 μmol of photons·m^{-2}·s^{-1}), and the PS II activity recovered to the initial level during the following 3 h in both strains. The decrease of PS II activity under high light in the presence of chloramphenicol and its recovery under dim light after the removal of chloramphenicol were almost the same in the wild type as those measured in the cells which did not experience chloramphenicol (Figure 3). In contrast, the ΔPsbU mutant was highly susceptible to photoinhibition if chloramphenicol was present, indicating that PS II was unstable without PsbU. After the removal of chlorampheni-

col, the PS II activity promptly recovered, showing that the biosynthesis system was normal. The results confirm that the stability of PS II was lost upon deletion of PsbU.

Electron Flow Assessed by Fluorescence Kinetics in Cells. Figure 4 shows fluorescence rise kinetics, which reflects the electron flow in the PS II reaction center. In the cells, the apparent levels of the initial (F_0) and maximal (F_m) fluorescence yields on a Chl basis increased in the ΔPsbU mutant compared to the wild type both in the presence and in the absence of DCMU (Figure 4A,C), implying that electron flow defects in the PS II reaction center had occurred in the ΔPsbU mutant. The fluorescence parameter, F_v/F_m, which reflects the PS II reaction center activity, was 0.40 in the wild type and 0.29 in the ΔPsbU mutant. The lower value of F_v/F_m in the ΔPsbU mutant suggests that water oxidation in PS II was also slowed in the mutant cells.

The effect of Cl^- depletion on the PS II electron flow was assessed since growth of the ΔPsbU mutant cells was highly reduced under Cl^--depleted conditions (Figure 2C). When the wild-type cells were grown under Cl^--depleted conditions, the fluorescence kinetics in the presence and
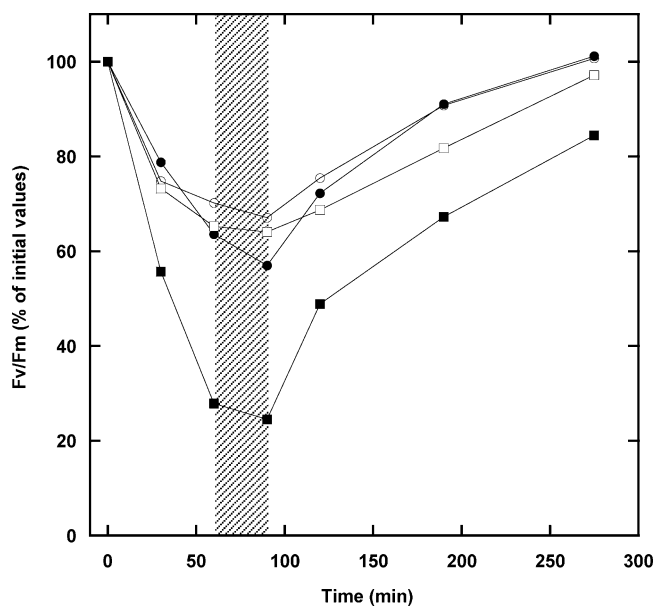
FIGURE 3: Sensitivity to photoinhibition. Cells (2 μg of Chl/mL) were exposed to 500 μmol of photons·m^{-2}·s^{-1} at 30 °C in the absence (open symbols) or presence (closed symbols) of 100 μg of chloramphenicol/mL, and F_v/F_m was measured. After a 60 min exposure to high light, the cells were washed twice to eliminate chloramphenicol and then incubated at 20 μmol of photons·m^{-2}·s^{-1} at 30 °C. The duration of the washing is shown as a shaded bar. Key: circle, wild type; square, ΔPsbU.

absence of DCMU (Figure 4B) were similar to those of the ΔPsbU mutant which was grown in normal BG11 medium (Figure 4C). This indicates that even wild-type cells could also suffer some effects on their electron flow under such conditions. However, the F_v/F_m value remained higher ($F_v/F_m = 0.35$) than that of ΔPsbU mutants grown in normal BG11 medium. In contrast, the effect of Cl$^-$ depletion was prominent in the ΔPsbU mutant. Both of the apparent F_0 and F_m levels increased in the ΔPsbU mutant, and the difference in fluorescence levels at time 0.1 s was very small with or without DCMU (Figure 4D), which reflects the low activity of the PS II reaction center ($F_v/F_m = 0.15$) under Cl$^-$-depleted conditions. Results similar to those of Figure 4 were obtained using PAM fluorometer with independent cell cultures although the fluorescence parameters somewhat varied. For example, the values of F_v/F_m were 0.396 ($\pm$0.013) and 0.310 ($\pm$0.001) for wild-type cells grown with or without Cl$^-$, respectively, and 0.348 ($\pm$0.009) and 0.286 ($\pm$0.009) for ΔPsbU cells grown with or without Cl$^-$, respectively ($n = 3$). The F_0 values were 6.91 ($\pm$0.163), 7.04 ($\pm$0.033), 7.04 ($\pm$0.188), and 8.70 ($\pm$0.496) (arbitrary units) for those cells, respectively.

Effect of Removal of psbU on the Steady-State Oxygen Evolution in Cells. Figure 5 shows the PS II-mediated oxygen evolution measured in cells grown in normal BG11 medium. The maximum rates of oxygen evolution under light-saturated conditions were approximately 60% and 30% that of wild-type cells in ΔPsbU and ΔPsbO cells, respectively. Under light-limiting conditions, the activities were constantly lower in ΔPsbU and even lower in ΔPsbO mutants than in the wild type. The photosynthetic parameters obtained from Figure 5 are summarized in Table 2. The efficiency of light utilization (α in Table 2) in ΔPsbU mutant cells was approximately 35% lower than that in wild-type cells [0.294 vs 0.449 [μmol of O$_2$/(mg of Chl·h)]/(μmol of

photons·m^{-2}·s^{-1})]. The ratio of these values is comparable to that of F_v/F_m (0.29 vs 0.40 for mutant and wild type, Figure 4A,C). In addition, the apparent maximum value of the activity (P_{max} in Table 2) was approximately 40% lower in ΔPsbU mutant cells than in wild-type cells [360 vs 588 μmol of O$_2$/(mg of Chl·h)]. The light intensity at which the photosynthesis begins to saturate (I_k in Table 2) was also lower in ΔPsbU mutants than in the wild type, indicating that in ΔPsbU the maximum light intensity at which the rate of water oxidation in PS II was able to follow the flux of incident light was highly reduced. This apparently impaired oxygen-evolving activity should not be attributed to the difference of the PS I/PS II ratio because the ratio was almost the same between these strains as observed from fluorescence emission spectra at 77 K (see below). This feature of the ΔPsbU mutant was different from that of the ΔPsbO mutant (Figure 5 and Table 2), in which the α, P_{max}, and I_k values were even smaller than in ΔPsbU. When the *psbU* gene was complemented, the light curve and, consequently, the photosynthetic parameters were restored to almost the same level as those of wild-type cells (Figure 5 and Table 2).

Effect of Removal of psbU on the Decay of S2 and S3 States. Since PsbU is located at the lumenal side of PS II complexes (6, 8, 9), the decay kinetics of S2 (Figure 6) and S3 states were measured to assess the intactness of the water-oxidizing machinery. The S2 state decayed apparently slower in the ΔPsbU mutant than in the wild type. On the other hand, the decay of the S3 state in ΔPsbU did not show a significant difference from that in the wild type (data not shown). The decay patterns of S2 states both in the wild type and in ΔPsbU were well fitted by double exponential decay ($R^2 > 0.999$) rather than a single exponential decay. The lifetimes and relative amounts of the two phases (fast and slow phases) in the S2 state are shown in Table 3. Interestingly, the lifetimes of the two components of S2 decay were the same in the wild-type and ΔPsbU cells. The relative amount of the slow component was markedly increased in the ΔPsbU mutant.

Effect of Removal of psbU on the Spectroscopic Properties of the Cells. Wild-type cells showed the Q$_y$ band of Chl peaking at 682 nm irrespective of the presence or absence of Cl$^-$ in the growth media (Figure S1, Supporting Information). However, the peak wavelengths originating from the Q$_y$ band of Chl in ΔPsbU cells grown under both normal BG11 and Cl$^-$-depleted conditions blue shifted by 1 nm from that of wild-type cells. The peak wavelengths of phycobilins were also blue shifted by 3 and 2 nm in the normal grown and Cl$^-$-depleted cells, respectively. When the wild-type and mutant cells were grown under Cl$^-$-depleted condition, the absorbance ratio of phycobilins to the Q$_y$ band of Chl increased compared to the cells grown in normal BG11.

The fluorescence emission spectrum of ΔPsbU cells at 77 K was identical to that of wild-type cells when they had been grown in normal BG11, indicating that the stoichiometry of PS II to PS I is almost the same in these strains if grown in normal BG11 (Figure S2, Supporting Information). The same result was obtained when the cells were illuminated by 420 nm light to exclusively excite Chls (data not shown). Additionally, because the cells were illuminated by light which can also excite phycobilins in this measurement, it is assumed that the absorption cross section is almost the same between these strains in this growth condition (Figure S2,
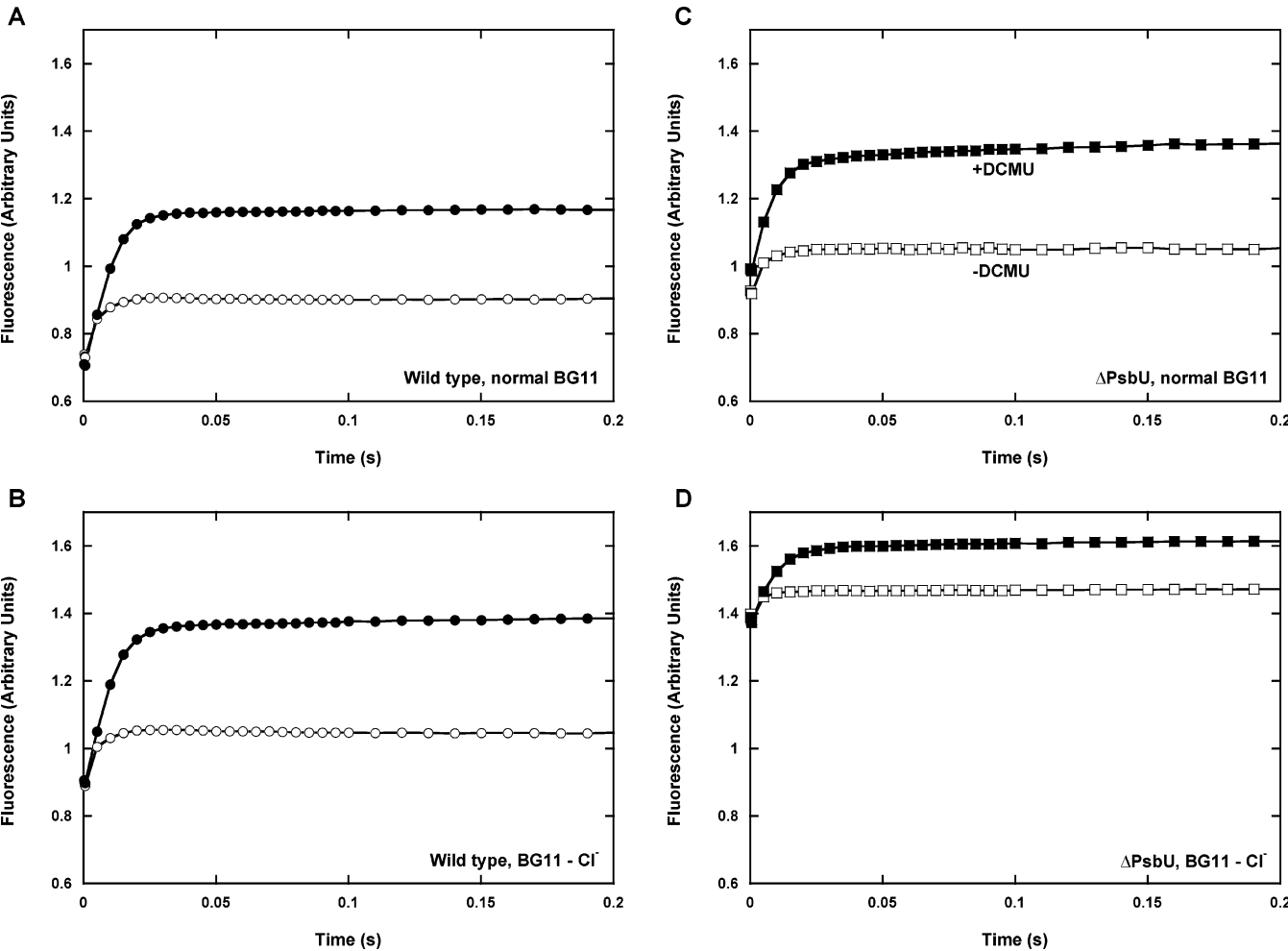
FIGURE 4: Fluorescence rise kinetics of cells grown in BG11 or BG11−Cl⁻ medium. Panels: A, wild-type cells grown in normal BG11; B, wild-type cells grown in BG11−Cl⁻; C, ΔPsbU cells grown in normal BG11; D, ΔPsbU cells grown in BG11−Cl⁻. Key: open symbols, no addition of DCMU; closed symbols, 20 μM DCMU. The samples were adjusted to 2 μg of Chl/mL.
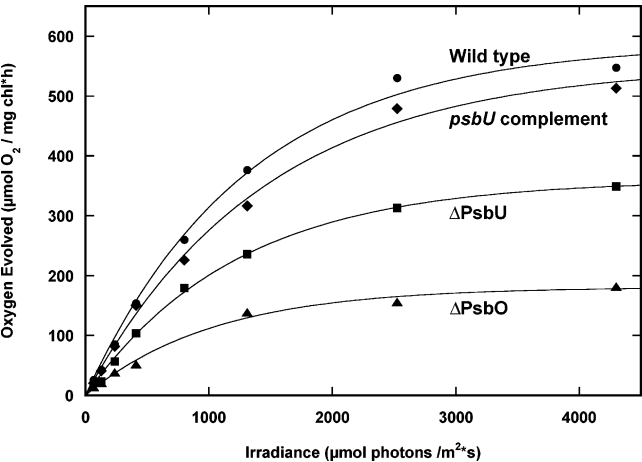

FIGURE 5: Effect of light intensity on steady-state oxygen evolution. Oxygen evolving activity was measured at 30 °C with 1 mM DCBQ as an electron acceptor. Data were fitted according to a model (*39*). Key: solid circle, wild type; solid square, ΔPsbU; solid triangle, ΔPsbO; solid diamond, complement of *psbU*.

Table 2: Photosynthetic Parameters Obtained from the Light Curves (Figure 5) for Cells Grown in Normal BG11 Medium[a]

	α	P_{max}	I_k
wild type	0.449	588	1300
ΔPsbU	0.294	360	1230
C-*psbU*	0.382	552	1440
ΔPsbO	0.174	181	1040

[a] α, [μmol of O$_2$/(mg of Chl·h)]/(μmol of photons·m^{-2}·s^{-1}). P_{max}, μmol of O$_2$/(mg of Chl·h). I_k, μmol of photons·m^{-2}·s^{-1}. C-*psbU*, complemented strain of ΔPsbU.

Supporting Information). When wild-type cells were grown under Cl⁻-depleted condition, the ratio of PS II to PS I, which can be roughly estimated by the ratio of peak heights at 696 and 727 nm, slightly increased. When ΔPsbU cells were grown under Cl⁻-depleted condition, the ratio of the peak height at ∼695 nm to that at 727 nm increased notably,

indicating the remarkable increase in the relative content of PS II to PS I. This was also observed when the cells were illuminated by light which was passed through a combination of 4-96 (Corning) and VR-42 (Toshiba, Tokyo, Japan) band-pass filters to specifically excite Chls. The emission from phycobilins increased in ΔPsbU cells of Cl⁻-depleted condition.

Effect of Removal of psbU on the Content of PS II and PS I Complexes. When wild-type cells were grown under Cl⁻-depleted condition, the relative amounts of CP47 and CP43 (peripheral Chl-binding proteins in PS II) to that of PsaA/B slightly increased compared to those in wild-type cells grown in normal BG11 (Figure S3, Supporting Information). These data are consistent with the result in Figure S2 (Supporting Information). The stainability of cyt *c*-550
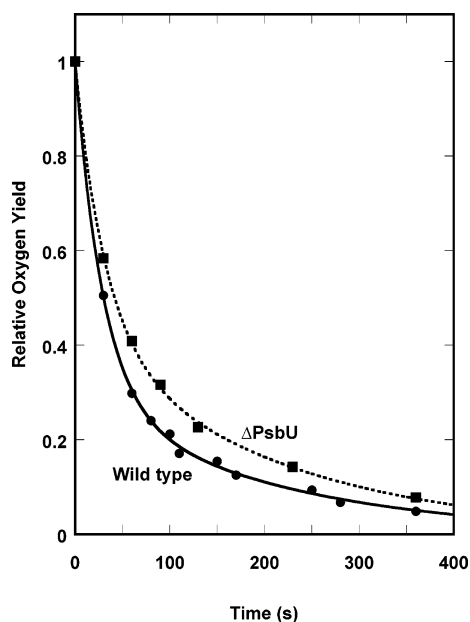
FIGURE 6: Decay kinetics of the S2 state in wild-type and ΔPsbU mutant cells grown in normal BG11 medium assessed by the measurement of oxygen flash yield. The decay kinetics are shown after normalization to the initial values. Key: solid circle, wild type; solid square, ΔPsbU.

Table 3: Lifetimes of S2 States Determined from Data Shown in Figure 6[a]

	half-lifetime (s)	relative content (%)
wild type	20 (1.3)	71 (3.0)
	140 (17)	29 (3.0)
ΔPsbU	22 (2.0)	57 (3.8)
	140 (14)	43 (3.8)

[a] The fast and slow components are listed. Numbers in parentheses are standard errors.

(PsbV) increased much more in the cells of Cl^--depleted condition. When ΔPsbU cells were grown in normal BG11 (Figure S3, lane C, Supporting Information), both Chl-specific amounts of PS II (CP47 and CP43) and PS I (PsaA/B) subunits decreased compared to those of wild-type cells grown in normal BG11, maintaining the PS II to PS I ratio at almost the same as that in wild-type cells. When ΔPsbU cells were grown under Cl^--depleted condition, the relative ratio of CP47 and CP43 to PsaA/B increased notably compared to that of normal-grown ΔPsbU cells (Figure S3, Supporting Information). Accordingly, the stained heme in cyt *c*-550 (PsbV) increased to a detectable level in ΔPsbU cells of Cl^--depleted condition. The Chl-specific amounts of both PS II and PS I in Cl^--depleted ΔPsbU cells were also lower than those of wild-type cells (Figure S3, Supporting Information).

The decrease of the Chl-specific amounts of both PS II and PS I was also observed in isolated thylakoid membranes (Figure S4, Supporting Information). All of the relative amounts of PsaA/B, CP47, and PsbO in thylakoids isolated from ΔPsbU cells grown in normal BG11 were lower than those in wild-type thylakoids (Figure S4, Supporting Information). Still, the relative content of PS II to PS I seems to be maintained in ΔPsbU cells at almost the same level of wild-type cells. The apparent low content of PsbO and cyt *c*-550 (PsbV) was observed corresponding to the low content of PS II complexes in ΔPsbU thylakoids (lane C vs lane A

Table 4: Cl^- Effects on O_2 Evolution in Isolated Thylakoid Membranes[a]

	rates of O_2 evolution [μmol of $O_2 \cdot$(mg of Chl)$^{-1} \cdot$h^{-1}]	
	wild type	ΔPsbU
30 mM NaCl	304 (5)	101 (3)
30 mM NaNO$_3$	190 (3)	61 (5)
no addition	221 (5)	5 (3)

[a] Oxygen-evolving activity was measured at 30 °C with 0.5 mM 2,5-DCBQ as an electron acceptor. The reaction mixture contained 50 mM MES−NaOH (pH 6.5), 10 mM $MgSO_4$, 5 mM $CaSO_4$, and 1 M betaine, and the Cl^- concentration was less than the detectable limit ($<20 \mu$M). When 30 mM NaCl was added, the measured Cl^- was 37.2 mM, and when 30 mM NaNO$_3$ was added, the measured Cl^- was less than the detectable limit ($<20 \mu$M). The Chl concentration was 10 μg/mL. Numbers in parentheses are standard errors ($n = 3$).

Table 5: Effects of Cl^- on O_2 Evolution during Preparation of Thylakoid Membranes[a]

		rates of O_2 evolution [μmol of $O_2 \cdot$(mg of Chl)$^{-1} \cdot$h^{-1}]
wild type	$+Cl^-$	227 (8)
	$-Cl^-$	97 (2)
ΔPsbU	$+Cl^-$	80 (7)
	$-Cl^-$	37 (0)

[a] Thylakoid membranes were prepared with ($+Cl^-$) or without ($-Cl^-$) Cl^- ion. Oxygen-evolving activity was measured at 30 °C with 0.5 mM 2,5-DCBQ as an electron acceptor. The reaction mixture contained 50 mM MES−NaOH (pH 6.5), 10 mM $MgCl_2$, 5 mM $CaCl_2$, and 1 M betaine, and the measured Cl^- concentration was 36.4 mM. The Chl concentration was 10 μg/mL. Numbers in parentheses are standard errors ($n = 3$).

in Figure S4, Supporting Information). If thylakoid membranes were washed in the absence of Cl^- but in the presence of SO_4^{2-}, cyt *c*-550 (PsbV) seemed to be partially lost both in wild-type and in ΔPsbU thylakoids (Figure S4, lanes B and D, Supporting Information, but see below).

Cl^- Effects on Oxygen Evolution in Isolated Thylakoid Membranes. Table 4 shows the rate of oxygen evolution in thylakoid membranes. The activity of thylakoid membranes isolated from the ΔPsbU mutant was lower than that of the wild type even when Cl^- ions were present in the reaction mixture. If Cl^-, which affected the growth rate of ΔPsbU cells much more than Ca^{2+}, was not added to the reaction mixture, the rate of oxygen evolution in mutant thylakoids was reduced to $<10\%$ compared to that measured in the presence of Cl^-, while 70% of activity was retained in the wild-type thylakoids. It is noteworthy that monovalent anion, NO_3^-, restored the activity to around 60% of that measured in the presence of Cl^- in ΔPsbU thylakoids while it did not increase the oxygen-evolving activity of wild-type thylakoids. Divalent anion, SO_4^{2-}, was unable to restore the activity in ΔPsbU thylakoids because all of the measurements in Table 4 were performed in the presence of 15 mM SO_4^{2-}.

Table 5 shows the rate of oxygen evolution in thylakoid membranes prepared with or without Cl^-. Even in wild-type thylakoids, the activity decreased to about 40% if prepared without Cl^- but in the presence of 15 mM SO_4^{2-}. The oxygen-evolving activity in ΔPsbU thylakoids also decreased to ~50% if prepared without Cl^-.

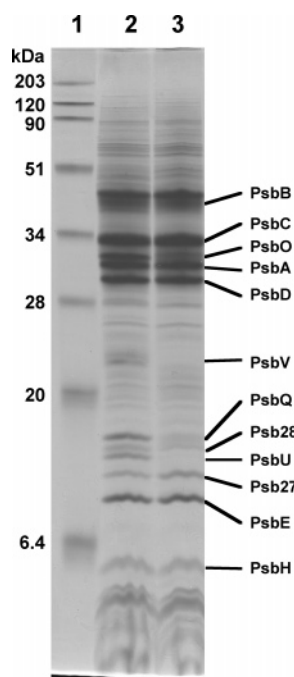*Polypeptide Profile of the PS II Core Complex.* PS II complexes were isolated from HT3 (*11*, *33*) and ΔPsbU/

FIGURE 7: Polypeptide profile of purified PS II complexes. Lanes: 1, molecular mass standards; 2, HT3−PS II complex; 3, ΔPsbU/HT3−PS II complex. Samples equivalent to 5 μg of Chl were loaded in each lane. The molecular mass of the standards is shown on the left. Bands were visualized by Coomassie blue staining.

Table 6: Relative Amounts of Extrinsic Polypeptides in Purified PS II Complexes[a]

	HT3	ΔPsbU/HT3
PsbO	+++	+
PsbV	+++	±
PsbU	+++	−
PsbQ	+++	+
Psb28	+++	+++
Psb27	+++	+++

[a] The relative amount of each protein band was estimated using the image processing program ImageJ (http://rsb.info.nih.gov/ij/index.html). Key: +++, original amount in HT3−PS II complexes or comparable amount (>70%) to the corresponding polypeptide in HT3−PS II; +, 40−20% of the corresponding polypeptide in HT3−PS II; ±, <20% of the corresponding polypeptide in HT3−PS II; −, absent.

FIGURE 8: Fluorescence rise kinetics of the PS II complexes purified from HT3 and ΔPsbU strains. Panels: A, PS II complexes isolated from HT3; B and C, PS II complexes isolated from ΔPsbU/HT3. Note that the time scale is different between panels B and C. Key: open symbols, no addition of DCMU; closed symbols, 20 μM DCMU. The samples were adjusted to 2 μg of Chl/mL.

HT3, and their polypeptide components were analyzed (Figure 7 and see ref *11*). HT3−PS II complexes showed a typical polypeptide profile (see ref *11*). As expected, PsbU was not detected in ΔPsbU/HT3−PS II complexes. It is notable that other extrinsic polypeptides such as PsbO, PsbV, and PsbQ also markedly decreased in ΔPsbU/HT3−PS II complexes (Table 6). No remarkable change was recognized in other PS II polypeptides.

Electron Flow Assessed by Fluorescence Kinetics in Purified PS II Complexes. PS II complexes purified from the HT3 strain showed a prompt increase of fluorescence in the presence of DCMU (Figure 8A). Without DCMU and artificial electron acceptors, the fluorescence increased slowly and reached F_m levels approximately 0.5 s after the onset of actinic light. In the PS II complex isolated from ΔPsbU/HT3, the fluorescence rise in the presence of DCMU was extremely slowed, starting at a higher apparent F_0 (Figure 8B,C). The fluorescence rise in the absence of DCMU and artificial electron acceptors was further decreased; it took 2 s until the fluorescence reached the F_m level after the onset
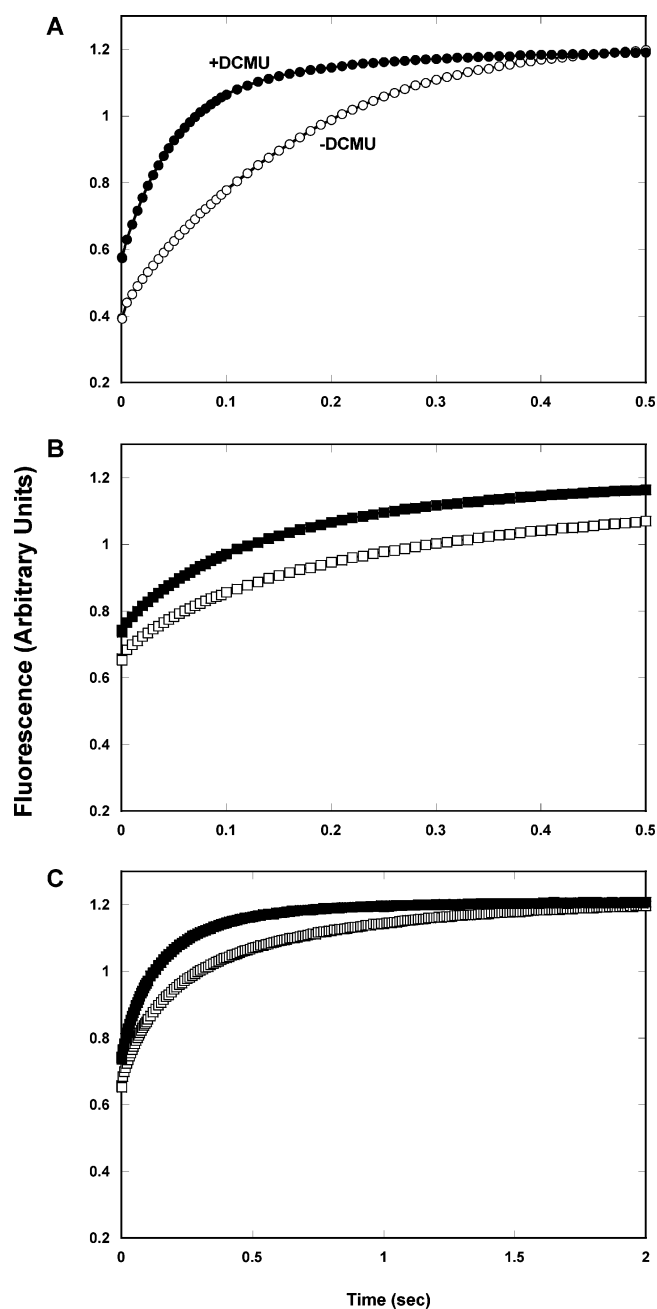
of actinic light (Figure 8B,C). These observations imply defects of electron donation from the water-oxidizing system in ΔPsbU.

DISCUSSION

Even without PsbU, the other three lumenal extrinsic proteins (PsbO, PsbQ, PsbV) might be able to associate with their own binding sites in PS II complexes in vivo. This can be deduced from the fact that the ΔPsbU mutant cells grew at almost the same rate as wild-type cells in normal BG11 medium (Figure 2A), although several defects were found that will be discussed later. Furthermore, unlike ΔPsbU

mutant cells, the double deletion mutant of *psbO* and *psbV* (ΔPsbO/ΔPsbV) did not grow even in the normal BG11 medium unless it was supplemented with glucose (data not shown, but see ref *48*). The light curve and the resulting photosynthetic parameters (Figure 5 and Table 2) also support the idea that other extrinsic proteins can associate with PS II complexes in vivo without the aid of PsbU. When the PsbO protein was lost from PS II, the values of α and P_{max} were decreased more than those in the ΔPsbU mutant (Table 2). Indeed, comparable amounts of PsbO (Figure S4, lane C, Supporting Information) and PsbQ (data not shown) were detected in isolated thylakoid membranes. The actual amount of PsbV remained ambiguous in this work because heme staining depends on the redox state and source of the heme (*36*, *49*).

Nonetheless, it was found that, in PS II complexes isolated from ΔPsbU mutants, a large amount of lumenal extrinsic proteins (PsbO, PsbQ, PsbV) were lost during the isolation process (Figure 7 and Table 6) despite the highly mild isolation method (*11*, *36*). This finding indicates that, without PsbU, the conformation of the water-oxidizing complex at the lumenal space of PS II (*6*) became highly fragile, leading to the slowed electron donation which was shown by the extremely decelerated fluorescence rise even in the presence of DCMU in isolated PS II (Figure 8B,C). Our current results revealed the structural importance of the PsbU protein in assisting the ordered conformational architecture of the water-splitting system. This contrasts with the previous studies, which reported that PsbU was not essential to PS II function (*21*, *22*).

Due to the loss of conformational stability of the water-oxidizing system and the decrease in the electron donation rate upon the deletion of PsbU, the mutant cells became highly sensitive to photoinhibition (Figure 3), which is consistent with the result reported by Clarke and Eaton-Rye (*50*). The structural function of PsbU also explains the result reported by Kimura et al. that the ΔPsbU mutant was more sensitive to heat stress than the wild type (*51*), although they argued that the PsbU protein, as well as the PsbO and PsbV proteins, stabilized the oxygen-evolving machinery against high-temperature stress.

Considering the function of PsbU described above, it is reasonable that the values of α, P_{max}, and I_k were notably reduced in ΔPsbU mutant cells compared to those in the wild-type cells (Table 2). Generally, when the α value decreased, three possibilities could be considered: (A) a decrease in the relative content of PS II, (B) a decrease in the antenna size of PS II, and (C) a decrease in the water oxidation rate in individual PS II. As discussed above, the observed property in the present ΔPsbU mutant belongs to the case of C. The low P_{max} and I_k in the ΔPsbU mutant cells can also be attributed to this low efficiency of water oxidation in PS II function. The former two possibilities (A and B) could be excluded because the fluorescence emission spectra indicated otherwise. When the ΔPsbU cells grown in normal BG11 were illuminated at 77 K with 420 nm light to exclusively excite Chls, the fluorescence spectrum was almost the same as that of the wild-type cells (data not shown). This indicates that the relative quantities of PS II to PS I are almost the same in both strains, which is consistent with the observation reported by Clarke and Eaton-Rye (*50*, *52*). When the cells grown in normal BG11 were

illuminated at 77 K by blue light which was passed through a 4-96 band-pass filter to excite both Chls and phycobilins (Figure S2, Supporting Information), the fluorescence spectra were almost identical in both strains, indicating that the energy distribution to photosystems was not so different between the two strains. The room temperature absorption spectra implied that the amount of phycobilins relative to Chls was maintained at almost the same level between the two strains when grown in normal BG11 (Figure S1, Supporting Information).

The room temperature absorption spectra revealed a blue shift of the peak wavelength by 1 nm around 685 nm in ΔPsbU cells (Figure S1, Supporting Information). This blue shift implies a decrease in the relative amount of Chls belonging to PS I. However, the relative content of PS II to PS I was almost identical between ΔPsbU and wild type as is described above (Figure S2, Supporting Information and refs *50* and *52*). Instead, the Chl-specific amount of subunit proteins belonging to both PS II and PS I decreased in ΔPsbU than those in wild type (Figures S3 and S4, Supporting Information). This suggests an increase in the amount of Chl-binding proteins which were degrading but still retaining Chls during the degradation process. This could result from the fragility of PS II complexes upon the deletion of PsbU. Actually, a broad smear was sometimes detected by antisera against Chl-binding proteins in ΔPsbU thylakoids (data not shown). The concomitant decrease of the content of PS I could be a result from the stoichiometric regulation in the cells. Then, the Chls bound to these degrading Chl-binding protein(s) will contribute to the increase of F_0 level, which was observed in Figure 4C. Furthermore, Clarke and Eaton-Rye (*50*, *52*) reported that the F_v/F_m value in ΔPsbU cells had been unusually smaller than that expected from the content of PS II although they had used hydroxylamine during the measurements. Their observation could also be explained by the increase in the degrading Chl-binding protein(s) and the resulting increase in the F_0 level. Some part of the decrease of P_{max} (Figure 5 and Table 2), but not α, in ΔPsbU cells could also be attributed to the increase in such Chls.

Shen et al. demonstrated that the peak temperatures of both the B and Q bands in thermoluminescence were increased by 4 °C in ΔPsbU mutant cells compared to those in wild-type cells, suggesting modification of the S2 state (*21*). In our analysis, the decay of the S2 state decelerated in ΔPsbU mutant cells compared to the wild-type cells (Figure 6). The decay kinetics of the S2 state consisted of two components (fast and slow phases) even in the wild-type cells (Table 3). Surprisingly, only the relative amount of the slow components was prominently increased in the ΔPsbU mutant, leaving the lifetimes of the two decay components unchanged, which could not be detected by the measurement of thermoluminescence (*21*). This indicates that PsbU supports normal S2 transition, and once PsbU is lost, a portion of the S2 state that has a redox potential lower (slow phase) than the normal S2 state (fast phase) becomes dominant (*53*, *54*), which could be inextricably linked, at least partly, to the low values of α and P_{max} in ΔPsbU cells (Figure 5 and Table 2).

The effect of Cl⁻ on the growth of ΔPsbU cells (Figure 2) was in distinct contrast to those reported earlier (*21*, *22*, *28*); the growth rate of ΔPsbU was largely suppressed under

Cl⁻-limited conditions in this study. We used plastic ware for the preparation of culture medium and the measurements of growth and excluded the possible contamination of ions. One of the reasons for the difference between studies may be the improved Cl⁻-limiting conditions achieved in this work. This is supported by the fact that the ΔPsbO mutant was unable to grow in our Cl⁻-limiting conditions although photoautotrophic growth under Cl⁻-limiting conditions had been reported (46). It is also possible that the discrepancy between studies may result from the difference in light intensity used in the two experiments. We used 50 μmol of photons·m⁻²·s⁻¹ for the measurement of growth, whereas Shen et al. used 30 μmol of photons·m⁻²·s⁻¹ (21, 22). The higher irradiance possibly affected PS II function more severely in the ΔPsbU mutant since the absence of PsbU caused fragility in the oxidizing side of PS II as discussed above (Figures 3 and 5 and Table 2).

On the basis of the results obtained here, we conclude that Cl⁻ can substitute the function of PsbU protein to some extent (Figure 2A,B), but Ca^{2+} cannot. Interestingly, the removal of Ca^{2+} from the growth medium together with Cl⁻ had an additional effect; the ΔPsbU mutant cells could not grow anymore, at least during the time tested, which is consistent with the report by Summerfield et al. (28). If the ΔPsbU cells were grown under Cl⁻-limited conditions (but in the presence of Ca^{2+}), the relative content of PS II increased (Figures S2 and S3, Supporting Information). However, the amount of active PS II was significantly decreased (Figure 4D). The decrease of the active PS II should have been partly compensated by the increase of PS II content. Again, the Chl-specific amounts of both PS II and PS I subunits decreased in ΔPsbU cells compared to those in wild-type cells if grown under Cl⁻-depleted condition (Figure S3, Supporting Information). This is also explained by the increase of the degrading Chl-binding proteins in ΔPsbU cells as is described above. The unusual increase in F_0 (Figure 4D) could be attributed to the Chls bound to degrading Chl-binding protein(s) and the increase of inactive PS II. It is interesting that the level of the stained cyt *c*-550 (PsbV) increased even in wild-type cells if they were grown under Cl⁻-depleted condition (Figure 2).

In addition, if Cl⁻ was depleted during the preparation of thylakoids, some part of cyt *c*-550 (PsbV) seemed to be lost (Figure S4, Supporting Information) and the oxygen-evolving activity decreased (Table 5). Instead, oxygen evolution was highly supported by Cl⁻ in isolated ΔPsbU thylakoid membranes as well as in wild-type thylakoids (Table 4). Interestingly, 60% of the activity was recovered by an addition of monovalent anion NO₃⁻ in ΔPsbU thylakoids, although a slight inhibitory effect was observed for wild-type thylakoids (Table 4). Different from NO₃⁻, a divalent anion, SO_4^{2-}, was not effective to restore the activity in ΔPsbU thylakoids (Table 4). The effect of monovalent cation, Na⁺, on the oxygen-evolving complex (55) could be neglected, because both Cl⁻ and NO₃⁻ were added as sodium salts, the pH of the reaction mixture was adjusted by NaOH, and 5 mM Ca^{2+} was present in all measurements. Therefore, we can distinguish two effects of Cl⁻ on PS II function. One is a generally accepted function to support the oxygen-evolving process (e.g., refs 10, 56, and 57) which was observed typically in wild-type thylakoids (Table 4). Another is a capability to substitute the function of PsbU when PsbU

is absent, which can also be achieved by other monovalent anions such as NO₃⁻. These results suggest that PsbU has some structural properties resembling to monovalent anion such as Cl⁻ and NO₃⁻, and both PsbU and Cl⁻ are important to keep the proper structural architecture of the oxygen-evolving system. Accordingly, we prefer the idea that PsbU may stabilize only Ca^{2+}, and not Cl⁻, through its structural nature although it is generally accepted that the PsbU protein may provide the binding site for Cl⁻ and Ca^{2+} ions (10, 23) as is thought for the PsbP or PsbQ proteins in higher plant PS II (10, 12, 24). This idea could also be supported by the structural information on PS II complexes from *Thermosynechococcus elongatus* (8). Since the three-dimensional structure of PS II from *T. elongatus* is now available (8; Protein Data Bank accession number 1S5L), we have depicted the structure of PsbU and evaluated the electrostatic property of PsbU, which may be a key feature to the binding of ions (data not shown), using Deep View [spdbv 3.7 (58)]. The huge negative potential is prominent around PsbU, which might be realized by Cl⁻ ions if PsbU is absent from the water-splitting system of PS II. This huge negative potential may contribute to maintain the optimal concentration of Ca^{2+} near the Mn cluster (59).

The effect of NO₃⁻ on the ΔPsbU thylakoids is a clear contrast with that on spinach PS II, in which NO₃⁻ takes the place of Cl⁻ but does not support a high rate of oxygen evolution (60, 61). Although spinach PsbP and PsbQ may constitute a diffusion barrier for the Cl⁻-binding site in spinach PS II (62), the difference between results (Table 4 and refs 60 and 61) is not attributed to the absence of PsbU in ΔPsbU thylakoids and the presence of PsbP and PsbQ in spinach PS II complexes. This is deduced from the result that only short time exposure of wild-type thylakoids to the Cl⁻-depleted and NO₃⁻-supplemented medium was enough for the substantial decrease in oxygen-evolving activity (Table 4). It is known that Br⁻ can fully substitute for Cl⁻ in spinach PS II (60, 61) and cyanobacterial cells (63). However, different from Br⁻, NO₃⁻ did not fully support the oxygen-evolving activity in ΔPsbU thylakoids (Table 4) and further the growth of ΔPsbU mutant under Cl⁻-limited condition at 18 mM NO₃⁻ (Figure 2C). In this sense, the action of NO₃⁻ to the cyanobacterial PS II may be different from the well-known function of Cl⁻ on the water oxidation reaction in PS II. The ionic radius of these monovalent anions may be responsible for these different effects on oxygen-evolving activity.

It is noteworthy that SO_4^{2-}, which is thought to be effective to deplete Cl⁻ from PS II (64), does not seem to inhibit the activity in the wild-type thylakoids at 15 mM in the presence of 30 mM Cl⁻ and also not so much in the absence of Cl⁻ (Table 4). This contrasts with the case in spinach PS II whose oxygen-evolving activity was totally lost by 1 mM MgSO₄ at a very low concentration of Cl⁻ (less than 1 μM free Cl⁻) (65), implying a different structural and functional architecture between cyanobacterial and higher plant oxygen-evolving complexes. Accordingly, the ΔPsbU strain will become a useful source to investigate the function of Cl⁻ and other anions on the oxygen-evolving complex in cyanobacterial PS II.

Through our investigation, it can be concluded that PsbU provides a stable structural architecture of the water-splitting system, and maybe electrostatic environment, to ensure a

smooth water oxidation process. This function of PsbU is different from that proposed for PsbP and PsbQ in plant chloroplasts to serve as binding sites for Ca^{2+} and/or Cl^- (*10*). This conflicts with the conventional model that PsbU and PsbV were replaced by PsbQ and PsbP during the evolutional process (*18, 19, 25, 26*) but is consistent with our recent model that PsbU and PsbV are present together with PsbQ and PsbP in cyanobacterial PS II complexes and have a different role(s) from PsbQ and PsbP (*27*).

Still, it is true that Ca^{2+} and Cl^- are necessary for effective water oxidation. With regard to the habitat of cyanobacteria, the physicochemical environment is highly variable, e.g., from seawater to freshwater (*66−68*). Oceanic cyanobacteria can import as much Ca^{2+} and Cl^- as they need because the concentration of Ca^{2+} is approximately 10 mM and that of Cl^- is around 0.6 M. However, for the freshwater cyanobacteria and land-living cyanobacteria, the availability of such ions might be limited and highly variable depending on their environments (*69*), for example, 0.05 mM Ca^{2+} and 0.14 mM Cl^- in very soft lake water or 4.5 mM Ca^{2+} and 4.2 mM Cl^- in very hard underground water. PsbU may play an important role to maintain an effective water oxidation under any salinity environment especially for the freshwater cyanobacteria and land-living cyanobacteria. In this sense, it is interesting that the two strains of marine *Prochlorophytes* do not carry genes homologous to *psbU* (*20*).

ACKNOWLEDGMENT

SUPPORTING INFORMATION AVAILABLE

Absoption spectra of cells at room temperature, fluorescence emission spectra of cells at 77 K, chlorophyll-specific amount of subunit proteins of PS II and PS I complexes in cells, and effect of Cl^- depletion during the preparation of thylakoid membranes. This material is available free of charge via the Internet at http://pubs.acs.org.

REFERENCES

1. Dekker, J. P., and Boekema, E. J. (2005) Supramolecular organization of thylakoid membrane proteins in green plants, *Biochim. Biophys. Acta 1706*, 12−39.
2. Jordan, P., Fromme, P., Witt, H. T., Klukas, O., Saenger, W., and Krauss, N. (2001) Three-dimensional structure of cyanobacterial photosystem I at 2.5 Å resolution, *Nature 411*, 909−917.
3. Ben-Shem, A., Frolow, F., and Nelson, N. (2003) Crystal structure of plant photosystem I, *Nature 426*, 630−635.
4. Kurisu, G., Zhang, H., Smith, J. L., and Cramer, W. A. (2003) Structure of the cytochrome b_6f complex of oxygenic photosynthesis: tuning the cavity, *Science 302*, 1009−1014.
5. Stroebel, D., Choquet, Y., Popot, J. L., and Picot, D. (2003) An atypical haem in the cytochrome b_6f complex, *Nature 426*, 413−418.
6. Kamiya, N., and Shen, J.-R. (2003) Crystal structure of oxygen-evolving photosystem II from *Thermosynechococcus vulcanus* at 3.7-Å resolution, *Proc. Natl. Acad. Sci. U.S.A. 100*, 98−103.
7. Zouni, A., Witt, H. T., Kern, J., Fromme, P., Krauss, N., Saenger, W., and Orth, P. (2001) Crystal structure of photosystem II from *Synechococcus elongatus* at 3.8Å resolution, *Nature 409*, 739−743.
8. Ferreira, K. N., Iverson, T. M., Maghlaoui, K., Barber, J., and Iwata, S. (2004) Architecture of the photosynthetic oxygen-evolving center, *Science 303*, 1831−1838.
9. Biesiadka, J., Loll, B., Kern, J., Irrgang, K.-D., and Zouni, A. (2004) Crystal structure of cyanobacterial photosystem II at 3.2 Å resolution: a closer look at the Mn-cluster, *Phys. Chem. Chem. Phys. 6*, 4733−4736.
10. Seidler, A. (1996) The extrinsic polypeptides of photosystem II, *Biochim. Biophys. Acta 1277*, 35−60.
11. Kashino, Y., Lauber, W. M., Carroll, J. A., Wang, Q., Whitmarsh, J., Satoh, K., and Pakrasi, H. B. (2002) Proteomic analysis of a highly active photosystem II preparation from the cyanobacterium *Synechocystis* sp. PCC 6803 reveals the presence of novel polypeptides, *Biochemistry 41*, 8004−8012.
12. Calderone, V., Trabucco, M., Vujicic, A., Battistutta, R., Giacometti, G. M., Andreucci, F., Barbato, R., and Zanotti, G. (2003) Crystal structure of the PsbQ protein of photosystem II from higher plants, *EMBO Rep. 4*, 900−905.
13. Ifuku, K., Nakatsu, T., Kato, H., and Sato, F. (2004) Crystal structure of the PsbP protein of photosystem II from *Nicotiana tabacum*, *EMBO Rep. 5*, 362−367.
14. Stewart, A. C., Siczkowski, M., and Ljungberg, U. (1985) Glycerol stabilizes oxygen evolution and maintains binding of a 9 kDa polypeptide in photosystem II particles from the cyanobacterium, *Phormidium laminosum*, *FEBS Lett. 193*, 175−179.
15. Stewart, A. C., Ljungberg, U., Åkerlund, H.-E., and Andersson, B. (1985) Studies on the polypeptide composition of the cyanobacterial oxygen-evolving complex, *Biochim. Biophys. Acta 808*, 353−362.
16. Kienzl, P. F., and Peschek, G. A. (1983) Cytochrome *c*-549—an endogenous cofactor of cyclic photophosphorylation in the cyanobacterium *Anacystis nidulans*?, *FEBS Lett. 162*, 76−80.
17. Krogmann, D. W., and Smith, S. (1990) Low potential cytochrome *c*550 function in cyanobacteria and algae, in *Current Research in Photosynthesis* (Baltscheffsky, M., Ed.) pp 687−690, Kluwer Academic Publishers, Dordrecht.
18. Shen, J.-R., Ikeuchi, M., and Inoue, Y. (1992) Stoichiometric association of extrinsic cytochrome *c*550 and 12 kDa protein with a highly purified oxygen-evolving photosystem II core complex from *Synechococcus vulcanus*, *FEBS Lett. 301*, 145−149.
19. Shen, J.-R., and Inoue, Y. (1993) Binding and functional properties of two new extrinsic components, cytochrome *c*-550 and a 12-kDa protein, in cyanobacterial photosystem II, *Biochemistry 32*, 1825−1832.
20. De Las Rivas, J., Balsera, M., and Barber, J. (2004) Evolution of oxygenic photosynthesis: genome-wide analysis of the OEC extrinsic proteins, *Trends Plant Sci. 9*, 18−25.
21. Shen, J.-R., Ikeuchi, M., and Inoue, Y. (1997) Analysis of the *psb*U gene encoding the 12-kDa extrinsic protein of photosystem II and studies on its role by deletion mutagenesis in *Synechocystis* sp. PCC 6803, *J. Biol. Chem. 272*, 17821−17826.
22. Shen, J.-R., Qian, M., Inoue, Y., and Burnap, R. L. (1998) Functional characterization of *Synechocystis* sp. PCC 6803 Δ*psb*U and Δ*psb*V mutants reveals important roles of cytochrome *c*-550 in cyanobacterial oxygen evolution, *Biochemistry 37*, 1551−1558.
23. Enami, I., Kikuchi, S., Fukuda, T., Ohta, H., and Shen, J.-R. (1998) Binding and functional properties of four extrinsic proteins of photosystem II from a red alga, *Cyanidium caldarium*, as studied by release-reconstitution experiments, *Biochemistry 37*, 2787−2793.
24. Miyao, M., and Murata, N. (1983) Partial disintegration and reconstitution of the photosynthetic oxygen evolution system. Binding of 24 kilodalton and 18 kilodalton polypeptide, *Biochim. Biophys. Acta 725*, 87−93.
25. Enami, I., Yoshihara, S., Tohri, A., Okumura, A., Ohta, H., and Shen, J.-R. (2000) Cross-reconstitution of various extrinsic proteins and photosystem II complexes from cyanobacteria, red algae and higher plants, *Plant Cell Physiol. 41*, 1354−1364.
26. Enami, I., Iwai, M., Akiyama, A., Suzuki, T., Okumura, A., Katoh, T., Tada, O., Ohta, H., and Shen, J.-R. (2003) Comparison of binding and functional properties of two extrinsic components, cyt *c*550 and a 12 kDa protein, in cyanobacterial PSII with those in red algal PSII, *Plant Cell Physiol. 44*, 820−827.
27. Thornton, L. E., Ohkawa, H., Roose, J. L., Kashino, Y., Keren, N., and Pakrasi, H. B. (2004) Homologs of plant PsbP and PsbQ proteins are necessary for regulation of photosystem II activity in the cyanobacterium, *Synechocystis* 6803, *Plant Cell 16*, 2164−2175.

28. Summerfield, T. C., Shand, J. A., Bentley, F. K., and Eaton-Rye, J. J. (2005) PsbQ (Sll1638) in *Synechocystis* sp. PCC 6803 is required for photosystem II activity in specific mutants and in nutrient-limiting conditions, *Biochemistry 44*, 805−815.

29. Ohta, H., Suzuki, T., Ueno, M., Okumura, A., Yoshihara, S., Shen, J.-R., and Enami, I. (2003) Extrinsic proteins of photosystem II, *Eur. J. Biochem. 270*, 4156−4163.

30. Stanier, R. Y., Kunisawa, R., Mandel, M., and Cohen-Bazire, G. (1971) Purification and properties of unicellular blue-green algae (order *Chroococcales*), *Bacteriol. Rev. 35*, 171−205.

31. Oka, A., Sugisaki, H., and Takanami, M. (1981) Nucleotide sequence of the kanamycin resistance transposon Tn*903*, *J. Mol. Biol. 147*, 217−226.

32. Schweizer, H. D. (1993) Small broad-host-range gentamycin resistance gene cassettes for site-specific insertion and deletion mutagenesis, *BioTechniques 15*, 831−834.

33. Bricker, T. M., Morvant, J., Masri, N., Sutton, H. M., and Frankel, L. K. (1998) Isolation of a highly active photosystem II preparation from *Synechocystis* 6803 using a histidine-tagged mutant of CP 47, *Biochim. Biophys. Acta 1409*, 50−57.

34. Horinouchi, S., and Weisblum, B. (1982) Nucleotide sequence and functional map of pE194, a plasmid that specifies inducible resistance to macrolide, lincosamide, and streptogramin type B antibodies, *J. Bacteriol. 150*, 804−814.

35. Kashino, Y., Koike, H., and Satoh, K. (2001) An improved sodium dodecyl sulfate-polyacrylamide gel electrophoresis system for the analysis of membrane protein complexes, *Electrophoresis 22*, 1004−1007.

36. Kashino, Y. (2003) Separation methods in the analysis of protein membrane complexes, *J. Chromatogr. B 797*, 191−216.

37. Kashino, Y., Enami, I., Satoh, K., and Katoh, S. (1990) Immunological cross-reactivity among corresponding proteins of photosystems I and II from widely divergent photosynthetic organisms, *Plant Cell Physiol. 31*, 479−488.

38. Porra, R. J., Thompson, W. A., and Kriedemann, P. E. (1989) Determination of accurate extinction coefficients and simultaneous equations for assaying chlorophylls *a* and *b* extracted with four different solvents: verification of the concentration of chlorophyll standards by atomic absorption spectroscopy, *Biochim. Biophys. Acta 975*, 384−394.

39. Webb, W. L., Newton, M., and Starr, D. (1974) Carbon dioxide exchange of *Alnus rubra*: a mathematical model, *Oecologia 17*, 281−291.

40. Young, A., McChargue, M., Frankel, L. K., Bricker, T. M., and Putnam-Evans, C. (2002) Alterations of the oxygen-evolving apparatus induced by a ^{305}Arg → ^{305}Ser mutation in the CP43 protein of photosystem II from *Synechocystis* sp. PCC 6803 under chloride-limiting conditions, *Biochemistry 41*, 15747−15753.

41. Meetam, M., Keren, N., Ohad, I., and Pakrasi, H. B. (1999) The PsbY protein is not essential for oxygenic photosynthesis in the cyanobacterium *Synechocystis* sp. PCC 6803, *Plant Physiol. 121*, 1267−1272.

42. Hirani, T. A., Suzuki, I., Murata, N., Hayashi, H., and Eaton-Rye, J. J. (2001) Characterization of a two-component signal transduction system involved in the induction of alkaline phosphatase under phosphate-limiting conditions in *Synechocystis* sp. PCC 6803, *Plant Mol. Biol. 45*, 133−144.

43. Burnap, R. L., and Sherman, L. A. (1991) Deletion mutagenesis in *Synechocystis* sp. PCC 6803 indicates that the Mn-stabilizing protein of photosystem II is not essential for O$_2$ evolution, *Biochemistry 30*, 440−446.

44. Bockholt, R., Masepohl, B., and Pistorius, E. K. (1991) Insertional inactivation of the *psbO* gene encoding the manganese stabilizing protein of photosystem II in the cyanobacterium *Synechococcus* PCC 7942, *FEBS Lett. 294*, 59−63.

45. Mayes, S. R., Cook, K. M., Self, S. J., Zhang, Z., and Barber, J. (1991) Deletion of the gene encoding the Photosystem II 33 kDa protein from *Synechocystis* sp. PCC 6803 does not inactivate water-splitting but increases vulnerability to photoinhibition, *Biochim. Biophys. Acta 1060*, 1−12.

46. Philbrick, J. B., Diner, B. A., and Zilinskas, B. A. (1991) Construction and characterization of cyanobacterial mutants lacking the manganese-stabilizing polypeptide of photosystem II, *J. Biol. Chem. 266*, 13370−13376.

47. Burnap, R. L., Shen, J. R., Jursinic, P. A., Inoue, Y., and Sherman, L. A. (1992) Oxygen yield and thermoluminescence characteristics of a cyanobacterium lacking the manganese-stabilizing protein of photosystem II, *Biochemistry 31*, 7404−7410.

48. Shen, J.-R., Burnap, R. L., and Inoue, Y. (1995) An independent role of cytochrome *c*-550 in cyanobacterial photosystem II as revealed by double-deletion mutagenesis of the *psbO* and *psbV* genes in *Synechocystis* sp. PCC 6803, *Biochemistry 34*, 12661−12668.

49. Vargas, C., McEwan, A. G., and Downie, J. A. (1993) Detection of c-type cytochromes using enhanced chemiluminescence, *Anal. Biochem. 209*, 323−326.

50. Clarke, S. M., and Eaton-Rye, J. J. (1999) Mutation of Phe-363 in the photosystem II protein CP47 impairs photoautotrophic growth, alters the chloride requirement, and prevents photosynthesis in the absence of either PSII-O or PSII-V in *Synechocystis* sp. PCC 6803, *Biochemistry 38*, 2707−2715.

51. Kimura, A., Eaton-Rye, J. J., Morita, E. H., Nishiyama, Y., and Hayashi, H. (2002) Protection of the oxygen-evolving machinery by the extrinsic proteins of photosystem II is essential for development of cellular thermotolerance in *Synechocystis* sp. PCC 6803, *Plant Cell Physiol. 43*, 932−938.

52. Clarke, S. M., and Eaton-Rye, J. J. (2000) Amino acid deletions in loop C of the chlorophyll *a*-binding protein CP47 alter the chloride requirement and/or prevent the assembly of photosystem II, *Plant Mol. Biol. 44*, 591−601.

53. Nixon, P. J., and Diner, B. A. (1992) Aspartate 170 of the photosystem II reaction center polypeptide D1 is involved in the assembly of the oxygen-evolving manganese cluster, *Biochemistry 31*, 942−948.

54. Putnam-Evans, C., Burnap, R., Wu, J., Whitmarsh, J., and Bricker, T. M. (1996) Site-directed mutagenesis of the CP 47 protein of photosystem II: alteration of conserved charged residues in the domain ^{364}E-^{444}R, *Biochemistry 35*, 4046−4053.

55. Waggoner, C. M., Pecoraro, V., and Yocum, C. F. (1989) Monovalent cations (Na$^+$, K$^+$, Cs$^+$) inhibit calcium activation of photosynthetic oxygen evolution, *FEBS Lett. 244*, 237−240.

56. Lindberg, K., and Andreasson, L. E. (1996) A one-site, two-state model for the binding of anions in photosystem II, *Biochemistry 35*, 14259−14267.

57. van Vliet, P., and Rutherford, A. W. (1996) Properties of the chloride-depleted oxygen-evolving complex of photosystem II studied by electron paramagnetic resonance, *Biochemistry 35*, 1829−1839.

58. Guex, N., and Peitsch, M. C. (1997) SWISS-MODEL and the Swiss-PdbViewer: an environment for comparative protein modeling, *Electrophoresis 18*, 2714−2723.

59. Adelroth, P., Lindberg, K., and Andreasson, L. E. (1995) Studies of Ca^{2+} binding in spinach photosystem II using ^{45}Ca^{2+}, *Biochemistry 34*, 9021−9027.

60. Ono, T., Nakayama, H., Gleiter, H., Inoue, Y., and Kawamori, A. (1987) Modification of the properties of S$_2$ state in photosynthetic O$_2$-evolving center by replacement of chloride with other anions, *Arch. Biochem. Biophys. 256*, 618−624.

61. Wincencjusz, H., Yocum, C. F., and van Gorkom, H. J. (1999) Activating anions that replace Cl$^-$ in the O$_2$-evolving complex of photosystem II slow the kinetics of the terminal step in water oxidation and destabilize the S$_2$ and S$_3$ states, *Biochemistry 38*, 3719−3725.

62. Wincencjusz, H., Yocum, C. F., and van Gorkom, H. J. (1998) S-state dependence of chloride binding affinities and exchange dynamics in the intact and polypeptide-depleted O$_2$ evolving complex of photosystem II, *Biochemistry 37*, 8595−8604.

63. Putnam-Evans, C., and Bricker, T. M. (1997) Site-directed mutagenesis of the basic residues ^{321}K to ^{321}G in the CP 47 protein of photosystem II alters the chloride requirement for growth and oxygen-evolving activity in *Synechocystis* 6803, *Plant Mol. Biol. 34*, 455−463.

64. Homann, P. H. (1988) Structural effects of Cl$^-$ and other anions on the water oxidizing complex of chloroplast photosystem II, *Plant Physiol. 88*, 194−199.

65. Itoh, S., and Uwano, S. (1986) Characteristics of the Cl$^-$ action site in the O$_2$ evolving reaction in PS II particles: Electrostatic interaction with ions, *Plant Cell Physiol. 27*, 25−36.

66. Paerl, H. W. (2000) Marine Plankton, in *Ecology of Cyanobacteria: Their Diversity in Time and Space* (Whitton, B., and Potts, M., Eds.) pp 121−148, Kluwer Academic Publishers, Dordrecht.

67. Oliver, R. L., and Ganf, G. G. (2000) Freshwater Blooms, in *Ecology of Cyanobacteria: Their Diversity in Time and Space*

(Whitton, B., and Potts, M., Eds.) pp 149−194, Kluwer Academic Publishers, Dordrecht.

68. Oren, A. (2000) Salts and Brines, in *Ecology of Cyanobacteria: Their Diversity in Time and Space* (Whitton, B., and Potts, M., Eds.) pp 281−306, Kluwer Academic Publishers, Dordrecht.

69. Sheir, L. L. (1976) *Corrosion*, Newnes-Butterworths, London.

70. Meunier, P. C. (1993) Oxygen evolution by photosystem II: The contribution of backward transitions to the anomalous behaviour of double-hits revealed by a new analysis method, *Photosynth. Res. 36*, 111−118.